SCIENCE CHINA
Information Sciences

• RESEARCH PAPER •

December 2023, Vol. 66 222305:1–222305:16
https://doi.org/10.1007/s11432-022-3750-5

Off-grid DOA estimation via a deep learning framework

Yan HUANG[1*], Yanjun ZHANG[1], Jun TAO[2*], Cai WEN[3], Guisheng LIAO[4] & Wei HONG[1]

[1]*State Key Lab of Millimeter Waves, Southeast University, Nanjing* 211100*, China;*
[2]*Key Laboratory of Underwater Acoustic Signal Processing of Ministry of Education, Southeast University, Nanjing* 210096*, China;*
[3]*School of Information Science and Technology, Northwest University, Xi'an* 710069*, China;*
[4]*National Key Lab of Radar Signal Processing, Xidian University, Xi'an* 710071*, China*

Received 30 November 2022/Revised 22 March 2023/Accepted 23 April 2023/Published online 13 November 2023

Abstract Direction-of-arrival (DOA) estimation problem is one of the most important tasks for array signal processing. Conventional methods are limited by either the computational complexity or the resolution. In this paper, a novel deep learning (DL) framework for super-resolution DOA estimation is developed, where the grid mismatch problem is fully considered into the DL DOA estimation and the offset between the real DOA and the discrete sampling grid is thereby trained as a part of the network output. Specifically, we first model the DOA estimation problem as a multi-classification task and obtain the on-grid estimation result with a resolution of 1° as the first output. Then we designed another regression module to estimate the offset between target angles and the corresponding grids. By combining both on-grid and offset estimation results, the accurate off-grid estimation is achieved. In addition, the method of fusing low-level features and high-level features by skip connection is adopted between the on-grid estimation module and the offset estimation module. The high-level features in the first part of the network are combined with the original input to improve the training speed and the estimation accuracy. Herein, our training dataset contains a large number of off-grid signal data, which is close to the practical application. Also, the utilization of the off-grid part information improves DOA estimation performance compared to existing DL-based methods, achieving more accurate DOA estimations. Numerous simulation results have demonstrated the superiority of the proposed method in DOA estimation precision, and a good performance advantage maintains even when using a limited number of snapshots. Further, we test the proposed method on the real millimeter-wave radar system, and it outperforms the other state-of-the-art methods, especially for two adjacent targets in the same range and Doppler bin.

Keywords direction-of-arrival (DOA) estimation, deep learning (DL), off-grid, array signal processing

Citation Huang Y, Zhang Y J, Tao J, et al. Off-grid DOA estimation via a deep learning framework. Sci China Inf Sci, 2023, 66(12): 222305, https://doi.org/10.1007/s11432-022-3750-5

1 Introduction

Direction-of-arrival (DOA) estimation is an important part of array signal processing. It is a very attractive research field due to the plethora of applications in radar, sonar, wireless communication, earthquake, and underwater detection [1]. The main goals of DOA estimation are to improve the estimation precision for a super-resolution result and to reduce computational complexity simultaneously.

After a long period of development, researchers have proposed many DOA estimation methods, for example, beam-forming [2]. Traditional DOA estimation approaches are mostly model driven and establish the parametric model of both incident signal directions and array outputs. Hence, the DOA estimation performance largely depends on the model accuracy [3]. During this period, subspace-based methods play an important role in these researches due to their excellent performance, high resolution, and good robustness. Among all previous subspace-based methods, the most representative ones are multiple signal classification (MUSIC) [4] and estimation of signal parameters via rotational invariance techniques

* Corresponding author (email: yellowstone0636@hotmail.com, jtao@seu.edu.cn)

(ESPRIT) [5]. Many variants and improved versions, such as the root MUSIC method, have been born on the basis of these two methods, yielding very successful examples [6–8]. Basically, these algorithms usually require a large number of snapshots, prior information on the number of signal sources, and a large amount of computation [9]. Also, their performance and applicability are limited by the array model.

During the past decade, sparse representation has been gradually matured and widely used in various fields, where DOA estimation is one of the key applications for sparse representation methods [10, 11]. The DOA estimation based on sparse representation can be separated into three main categories. The first category is the on-grid method, including ℓ_1-SVD [12], sparse Bayesian learning (SBL) [13,14], sparse recovery for weighted subspace fitting (SRWSF) [15]. All of the above methods assume that the DOAs of the incident signals are located on a series of predefined angular grids. But in practice, the deviation between the true DOAs and the discretized sampling grids always exists. Since the DOAs are not exactly located at the fixed grids, their DOA estimation performance will degrade. Using sufficiently dense sampling grids can improve the accuracy, but the attendant problem is the increase of computational burden [16]. The other two categories of methods can eliminate or reduce this error [17], namely, off-grid methods [18–25] and gridless methods [26, 27]. Gridless methods directly estimate the DOAs in the continuous domain, which has better performance and much higher computational complexity. Also, they are typically limited to a uniform linear array (ULA) or a sparse linear array (SLA) [11].

The off-grid methods still need discrete sampling grids, but the influence of grid mismatch is further considered. In [18], it is assumed that the disturbance caused by grid mismatch is Gaussian distribution, and a sparse total least square (STLS) algorithm is proposed to solve the disturbance. However, this assumption does not meet the practical problem of off-grid DOA estimation. Then, a new off-grid sparse Bayesian inference (OGSBI) algorithm, which formulates the off-grid problem based on a Bayesian perspective, is introduced in [19]. The grid offset is assumed to satisfy a uniform prior model, which is based on a first-order Taylor series expansion. However, the computational time will increase greatly when using a finer grid. Inspired by this, the simultaneous orthogonal matching pursuit least-square (SOMP-LS) algorithm is proposed in [20] to estimate the off-grid DOAs by using a first-order Taylor series expansion model. In [21], the off-grid model is extended from first-order to second-order Taylor approximation based on the noise subspace fitting (NSF). As a result, more accurate DOA estimation is achieved through higher modeling accuracy. In [22], a method termed off-grid block sparsity Bayesian learning (OGBSBL) is formulated. Herein, a new off-grid model based on the sample covariance matrix with the off-grid representation of the steering vector is proposed and the block sparse Bayesian algorithm is employed to estimate the off-grid DOAs. Above all, the aforementioned off-grid DOA estimation methods still have two main limitations: on the one hand, these methods need to tune many parameters during the estimation process, which strongly affects the results of DOA estimation; on the other hand, the contradiction between computational time and estimation accuracy still exists, that is, more dense grids are required to obtain more accurate estimations, causing massive computations [17]. Then, the methods of grid refinement are proposed [24, 25] to improve the estimation accuracy by adaptively adjusting the rough grid, solving the contradiction between grid density and computation. However, the computational complexities of these methods are still quite high and can hardly be applied in practical applications.

In addition, machine learning techniques are also introduced into DOA estimation problems, such as support vector classification (SVC) [28], support vector regression (SVR) [29–32] and radial basis function (RBF) [33]. A method of DOA estimation based on SVC is introduced in [28]. In this paper, a multi-level technique is used to solve the large scale multi classification problem, but this method needs to train the classifier with the square number of categories. In [29], it is proposed to use SVR to fit the angle of arrival according to the signal covariance matrix. However, in the case of multiple signals, it is necessary to build a number of support vector machines (SVMs) equal to the number of signals. The author in [30] formulated SVM with minimum variance distortionless response (MVDR) and proposed SVM-MVDR and SVM-MUSIC to estimate the DOAs of incident waves. Similarly, a method combining SVR and forward-backward linear prediction (FBLP) is proposed in [31], but the experimental results show that the method performs poorly when estimating targets with very close angles. Recently, deep learning (DL), as a high-performance data-driven framework [34], has been widely used in various fields. The important application fields of DL include computer vision (CV) and natural language processing (NLP). Many classic neural network models appear, such as ResNet [35], recurrent neural network (RNN) [36], long short-term memory (LSTM) network, and you only look once (YOLO) [37]. In addition, DL has also been applied to various parameter estimation problems, including wireless communication and radar [38],

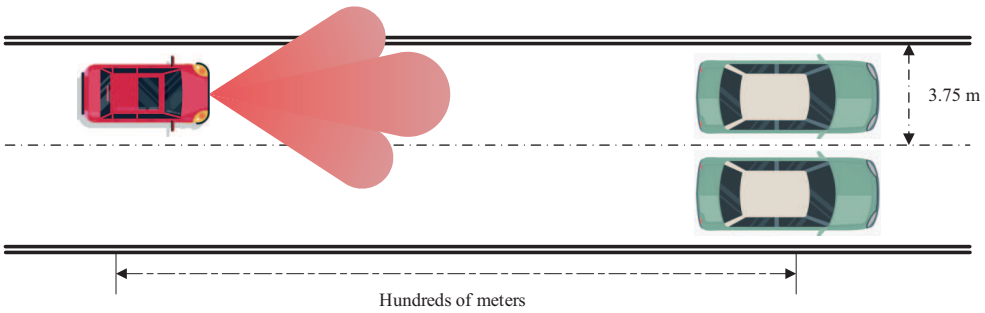

Figure 1 (Color online) Long distance target detection scene requiring high resolution.

and has achieved very good results. In wireless communication systems, DOA estimation is often used to aid channel estimation. At this point, to better convey information, a deep neural network (DNN)-based network [39] and a deep convolutional neural network (CNN)-based network [40] have been proposed. For DOA estimation of radar systems, the purpose is target sensing, hence there are higher requirements for accuracy, super resolution, and real-time performance. Considering these aspects, DL methods have many unique advantages. First, DL does not need to build a model, but directly learns the nonlinear relationship between array outputs and source DOAs from received data instead. Therefore, many problems caused by inaccurate models can be avoided, and higher accuracy can be maintained under various defect conditions. Second, as a data-driven method, the interval of source DOAs has little impact on it, enabling super-resolution estimation. Finally, after the network training, the estimates can be obtained quickly by simple calculations [38]. Compared with conventional methods, it has absolute advantages in low computational power systems and is more in line with the real-time requirement of practical applications.

A DNN composed of fully connected (FC) layers was employed in [41] for DOA estimation of two targets. However, the network is difficult to estimate correctly when the two targets are very close. The authors in [42] proposed a CNN for DOA estimation with a one-dimensional convolution filter. It shows some advantages in the case of low signal-to-noise ratio (SNR), but the overall performance is not greatly improved. Another CNN framework for DOA estimation was introduced in [43], the author also focused on the case of low SNRs. Although the estimation performance of the proposed network is further improved in the case of low SNRs, however, it is still an on-grid method in essence, and its performance will be limited in the case of high SNRs. Autoencoder (AE) is also widely used in DOA estimation to deal with the problem of array imperfections. The authors in [44] proposed a DNN framework based on a multi-task AE and multiple parallel classifiers, where the network does show robustness to array imperfections, but only a single SNR situation is considered during training and testing, which may not match the practical applications. Another deep AE for DOA estimation with array errors was published in [45], and the influence of coherent sources was further considered.

However, almost all the existing DOA estimation methods based on the DL model regard the problem as a multi-label classification task and they can still be regarded as on-grid methods. Most of them are estimated on a predetermined grid with 1° resolution. Also, only the signals with integer incident angles are used as training data, which directly ignores the information of the off-grid part or the so-called decimal-degree part. For actual scenarios, this not only leads to a certain degree of information loss but also is not suitable for occasions with higher accuracy requirements. For example, for long-distance target detection, as shown in Figure 1, to distinguish vehicles in adjacent lanes hundreds of meters away, the resolution achieved by the previous method is not enough. For these methods, estimation resolution can only be improved by using a finer grid. However, the cost of doing this is very high, which means that the length of the network output will be greatly increased. Then the network depth and a large number of parameters are required to increase to extract deeper features. In this way, the training cost of the network becomes unbearable, and it is difficult to get good results in so many categories of classification tasks. In addition, this is still an on-grid idea.

To the best of our knowledge, no specific DL-based technique was developed for off-grid DOA estimation. Moreover, in practice, the incident angle of the signal does not exactly fall on a discrete grid, and the accuracy of existing grid based estimation methods cannot meet some high-resolution application scenarios, such as remote target detection and point cloud imaging. Hence, in this paper, we propose a DL framework for off-grid DOA estimation, which mainly consists of two parts. The first part is the multi-label classification task. Through parameter learning and the powerful nonlinear mapping ability

of the neural network, the input is mapped to the grid, and the estimation result of signal incidence angle on the rough grid is obtained. The second part is a regression task. Based on the estimation results in the first part, the offset between the signal angle and the grid is further obtained. Combining the two outputs, i.e., adding the information of the off-grid part to the determined grid to optimize the estimation results and improve the estimation accuracy. The experimental results show that after considering the more practical signal situation and processing the off-grid part with the proposed method, higher resolution DOA estimation can be realized. The main contributions of this paper can be summarized as follows.

(1) We consider the grid mismatch problem in the DOA estimation method based on DL, and the proposed method contains two tasks. On the one hand, find the grid point closest to the target DOA on the predefined discrete grid, which is still a multi-label classification task to obtain a rough estimate of the signal DOAs. The other is to estimate the offset between the real signal DOA and the grid. This part is modeled as a regression task, because the offset to be estimated is a continuous value, which is more consistent with the actual situation. Therefore, the accuracy of DOA estimation is no longer limited to the determined discrete grids, and there is no need to use finer grids to improve the estimation performance, which relieves the difficulty of training.

(2) We design a multi-output network structure to estimate the grid points corresponding to the target DOAs and the deviation from the grid at the same time. The network consists of two parts, the original scheme of multi-label classification task is retained as the first part of the network to obtain a rough but reliable result on the grid. Then, in the second part of the whole network, the processing of off-grid information is modeled as a regression task, and the output directly represents the offset between the source angle and the grid. As a result, it presents the information of source DOA on both integer-degree grid and off-grid at the same time. By combining the two outputs, i.e., by adding the information of the off-grid part to the determined grid, the proposed scheme optimizes the estimation results and further improves the estimation accuracy.

The rest of this paper is organized as follows: Section 2 presents the basic signal model of a linear array for DOA estimation. In Section 3, we detail the data pre-processing methods and the proposed network. In Section 4, the experimental parameters are described and numerous experiments are given to demonstrate the effectiveness and robustness of the proposed method, and Section 5 concludes our work.

Notations. Before introducing the main body of this paper, we denote a set by Greek alphabet, e.g., χ, and its cardinality is $|\chi|$; matrices are denoted by boldface capital letters, e.g., $\boldsymbol{A}$; vectors are denoted by boldface lowercase letters, e.g., $\boldsymbol{a}$; and scalars are denoted by the lowercase letters, e.g., a. The imaginary unit is j ($\mathrm{j}^2 = -1$). The transpose of a matrix is $[\cdot]^{\mathrm{T}}$ and the conjugate transpose of a matrix is $[\cdot]^{\mathrm{H}}$. $\boldsymbol{I}_N$ is the $N \times N$ identity matrix. The symbol $\mathrm{E}[\cdot]$ is the expectation operator.

2 Signal model

In this paper, we consider a standard signal model for DOA estimation [46,47]. Assume that K far-field narrowband sources with complex amplitudes $s_k(t)$ impinge on the N-element array from direction θ_k, where $k = 1, 2, \ldots, K$. Then the received signal at time t is

$$\boldsymbol{y}\left(t\right) = \sum_{k=1}^{K} \boldsymbol{a}\left(\theta_k\right) s_k\left(t\right) + \boldsymbol{n}\left(t\right), \quad t = 1, \ldots, T, \tag{1}$$

where T is the number of snapshots, $\boldsymbol{a}(\theta_k)$ denotes the steering vector corresponding to θ_k and $\boldsymbol{n}(t) \in C^{N\times 1}$ denotes the noise vector. Without loss of generality, we consider a ULA configuration for simplicity, so the steering vector can be expressed as

$$\boldsymbol{a}(\theta_k) = [1, \mathrm{e}^{\mathrm{j}\frac{2\pi d}{\lambda}\sin(\theta_k)} \cdots \mathrm{e}^{\mathrm{j}\frac{2\pi d}{\lambda}\sin(\theta_k)(N-1)}]^{\mathrm{T}}, \tag{2}$$

where d is the array element spacing and λ is the wavelength.

Defining the $N \times K$ array manifold matrix $\boldsymbol{A}(\theta) = [\boldsymbol{a}(\theta_1),\boldsymbol{a}(\theta_2), \ldots,\boldsymbol{a}(\theta_K)]$, we can rewrite (1) as

$$\boldsymbol{y}\left(t\right) = \boldsymbol{A}(\theta)\boldsymbol{s}(t) + \boldsymbol{n}(t), \quad t = 1, \ldots, T, \tag{3}$$

The covariance matrix of received signal $\boldsymbol{y}(t)$ can be expressed as

$$\boldsymbol{R}_y \triangleq \mathrm{E}[\boldsymbol{y}(t)\boldsymbol{y}^{\mathrm{H}}(t)] = \boldsymbol{A}(\theta)\boldsymbol{R}_s\boldsymbol{A}^{\mathrm{H}}(\theta) + \boldsymbol{R}_N. \tag{4}$$

Herein, we assume that all the impinging signals and noise components are mutually uncorrelated and have the same power. The signal covariance matrix $\boldsymbol{R}_s$ and noise covariance matrix $\boldsymbol{R}_N$ are given by

$$\boldsymbol{R}_s = \mathrm{E}[\boldsymbol{s}(t)\boldsymbol{s}^{\mathrm{H}}(t)], \tag{5}$$

$$\boldsymbol{R}_N = \mathrm{E}[\boldsymbol{n}(t)\boldsymbol{n}^{\mathrm{H}}(t)] = \sigma_{_N}^2\boldsymbol{I}_N. \tag{6}$$

Also, the signal $\boldsymbol{s}(t)$ is supposed to be uncorrelated with noise $\boldsymbol{n}(t)$, therefore, $\mathrm{E}[\boldsymbol{s}(t)\boldsymbol{n}^{\mathrm{H}}(t)] = \mathrm{E}[\boldsymbol{s}^{\mathrm{H}}(t)\boldsymbol{n}(t)] = 0$. By fully considering the above assumptions, the covariance matrix of the received signal can be rewritten as

$$\boldsymbol{R}_y \triangleq \mathrm{E}[\boldsymbol{y}(t)\boldsymbol{y}^{\mathrm{H}}(t)] = \boldsymbol{A}(\theta)\boldsymbol{R}_s\boldsymbol{A}^{\mathrm{H}}(\theta) + \sigma_n^2\boldsymbol{I}_N. \tag{7}$$

Actually, in practical applications, we are unable to obtain this ideal covariance matrix in (7). Commonly, the covariance matrix is required to be estimated with the received data of T snapshots, that is,

$$\hat{\boldsymbol{R}}_y = \frac{1}{T}\sum_{t=1}^{T}\boldsymbol{y}(t)\boldsymbol{y}^{\mathrm{H}}(t). \tag{8}$$

As mentioned before, we hope to obtain the super-resolution estimation of DOAs of unknown sources from the received signal. The covariance matrix of the received signal contains a lot of information, and the amount of data is greatly reduced compared with the received signal itself. As an important tool to analyze the received signal, the covariance matrix is used as the input of our network to extract the features from received signals.

3 Off-grid DOA estimation with DL

In this section, we propose a two-part DNN framework, which is used to estimate the DOAs of the target signals on a 1° resolution grid and process the information of the off-grid part. Then combining the estimation results of the two parts, we can achieve higher accuracy DOA estimation.

3.1 Algorithm analysis and motivation

A common idea for DOA estimation of array signals is to use the signal covariance matrix estimated in (8), including traditional super-resolution algorithms and many existing DL-based algorithms. The covariance matrix contains the information of the wave-path difference caused by the signal incident on the array elements at different positions. Through calculation and processing, we can obtain the signal incident angle we are interested in. Without generality, take the MUSIC method as an example, it performs eigenvalue decomposition (EVD) on the covariance matrix to obtain the signal subspace and noise subspace

$$\boldsymbol{R}_y = \boldsymbol{V}\boldsymbol{\Lambda}\boldsymbol{V}^{\mathrm{H}}, \tag{9}$$

where $\boldsymbol{V}$ is an $N \times N$ matrix of eigenvectors of $\boldsymbol{R}_y$ that can be divided into signal subspace and noise subspace and $\boldsymbol{\Lambda}$ is a diagonal matrix composed of the corresponding eigenvalues. In theory, K eigenvectors in $\boldsymbol{V}$ corresponding to K larger eigenvalues in $\boldsymbol{\Lambda}$ represent the signal subspace $\boldsymbol{V_S}$, and $N-K$ eigenvectors in $\boldsymbol{V}$ corresponding to $N-K$ smaller eigenvalues in $\boldsymbol{\Lambda}$ represent the noise subspace $\boldsymbol{V_N}$. Then, the MUSIC method uses noise subspace to construct a spatial spectrum, which can be expressed as

$$\mathrm{P}_{\mathrm{MUSIC}}(\theta) = \frac{1}{\boldsymbol{a}^{\mathrm{H}}(\theta)\boldsymbol{V_N}\boldsymbol{V_N}^{\mathrm{H}}\boldsymbol{a}(\theta)}. \tag{10}$$

The DOA estimation result of the MUSIC method can be obtained by searching the peak value of $\mathrm{P}_{\mathrm{MUSIC}}(\theta)$ in the whole angle search rang $[\phi_{\min}, \phi_{\max}]$, which can be expressed as

$$\hat{\theta} = \underset{\theta\in[\phi_{\min},\phi_{\max}]}{\arg\max}\ \mathrm{P}_{\mathrm{MUSIC}}(\theta), \tag{11}$$

The covariance matrix of the received signal contains information about the spatial dimension that is easy to extract, and it is also the most commonly used input form of previous DL methods. Take the processing flow of the above MUSIC algorithm as an example, the EVD operation can be regarded as a nonlinear mapping operation to extract noise subspace from covariance matrix, i.e., $\boldsymbol{V_N} = \mathcal{F}_1(\boldsymbol{R}_y)$. Similarly, the subsequent process of constructing a spatial spectrum can also be seen as a nonlinear projection. Searching for the maximum peak and obtaining the angle estimation result can be regarded as the ReLU activation function in the neural network, which is formulated as $\hat{\theta} = \mathcal{F}_2(\boldsymbol{V_N})$. A multi-layer neural network can accomplish these tasks well and achieve end-to-end nonlinear fitting.

Previous research studies have shown that neural networks can realize the transformation from the covariance matrix to the spatial spectrum [42, 48, 49], or realize end-to-end DOA estimation with the covariance matrix [41, 43]. The first part of the scheme proposed in this paper is also similar to them. Through a multi-layer neural network, the position of the signal angle on a predetermined discrete grid is obtained from the covariance matrix. Furthermore, on this basis, we want to estimate the offset between the signal and these discrete points, so as to improve the estimation accuracy. As far as we know, there is no DL-based method to solve the problem from this perspective.

First, estimating the offset between the target and the grid is a more difficult task, because it requires higher resolution. The original input data contains unprocessed high-resolution information, which is necessary for estimating details such as grid offset, and can enhance the resolution of adjacent targets, so it is an appropriate choice as part of the input. On the other hand, the high-level features obtained after network processing in the first part provide low resolution but more accurate information, which is very close to the estimation results on the grid, and can improve the training efficiency. Also, the estimation of grid offset should be based on the grid-based estimation results, so the high-level features in the first part of the network should also be contained in the input of the second part. Here, a skip connection is introduced to add the high-level features extracted in the first part to the input of the second part. As a result, it can be seen as further determining the specific position of the target near the grid point found in the first part of the network. Finally, the offset between the target and the grid should be a continuous value, so this part of the problem is modeled as a regression task, and the output length corresponds to the number of targets. Similarly, another multi-layer neural network is used to complete this part of the task.

3.2 Data preprocessing

As mentioned above, we intend to extract features from the covariance matrix of the received signal and estimate the DOAs. Since the covariance matrix is a Hermitian matrix, the information contained in the upper-triangle and lower-triangle parts of the covariance matrix is highly repetitive. So as to reduce the duplication of information and shorten the size of input data, we only use the data of the main diagonal and lower-triangular parts. Also, it is required to take the real and imaginary parts of each entry of the covariance matrix except for the diagonal elements as the input. Therefore, the input vector of the DNN is written as

$$\boldsymbol{x} = [\tau_{1,1}, \ldots, \tau_{N,N}, \Re(\tau_{2,1}), \Im(\tau_{2,1}), \Re(\tau_{3,1}), \Im(\tau_{3,1}), \ldots, \Re(\tau_{N,N-1}), \Im(\tau_{N,N-1})]^{\mathrm{T}}, \tag{12}$$

where $\tau_{i,j}$ denotes the (i,j)-th element of the correlation matrix with $i,j \in \{1,2,\ldots,N\}$. Herein, $\Re(\cdot)$ and $\Im(\cdot)$ represent the real and imaginary parts, respectively. Therefore, the input is an $N^2 \times 1$ vector.

First, like previous DL-based methods, we estimate the DOAs of the target signals on a 1° resolution grid. Suppose that the search range is $[\phi_{\min}, \phi_{\max}]$, the number of output units becomes $\phi_{\max} - \phi_{\min} + 1$ and each output value is within the range $[0,1]$. For example, the angle search range is from $\phi_{\min} = -60^\circ$ to $\phi_{\max} = 60^\circ$, then the grid map is $\eta = \{-60^\circ, \ldots, -1^\circ, 0^\circ, 1^\circ, \ldots, 60^\circ\}$. So the angle pair $\{-60^\circ, -58^\circ\}$ corresponds to a 121×1 binary vector $\boldsymbol{z}_1 = [1,0,1,0,\ldots,0]^{\mathrm{T}}$, which serves as the corresponding output or label of the first part of proposed network. Regarding the second part, the remaining off-grid information needs to be processed and we model this part as a regression task. Therefore, the output length is equal to the number of impinging sources K. As shown in Figure 2, the second output is to represent the offset between the target DOAs and the grid. For example, suppose that two sources impinge onto the array from directions θ_1 and θ_2, their offset from the grid is $(\theta_1 - [\theta_1]_r)$ and $(\theta_2 - [\theta_2]_r)$, where the $[\cdot]_r$ denotes the round operation. In order to facilitate processing and training, the original value in $[-0.5, 0.5)$ is expanded to $[-50, 50)$, so the corresponding output/label to the second part of the proposed network is $\boldsymbol{z}_2 = (\theta_1 - [\theta_1]_r, \theta_2 - [\theta_2]_r) \times 100$. Hence, the i-th training sample consists of data pairs in the

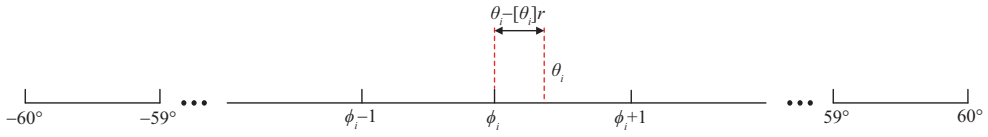

Figure 2 (Color online) Schematic diagram of label setting.

form $\{\boldsymbol{x}^i, \boldsymbol{z}_1^i, \boldsymbol{z}_2^i\}$, including one input and two labels. Therefore, a dataset containing D samples can be expressed as $\boldsymbol{D} = \{(\boldsymbol{x}^1, \boldsymbol{z}_1^1, \boldsymbol{z}_2^1), (\boldsymbol{x}^2, \boldsymbol{z}_1^2, \boldsymbol{z}_2^2), \ldots, (\boldsymbol{x}^D, \boldsymbol{z}_1^D, \boldsymbol{z}_2^D)\}$.

3.3 Network framework

In the whole framework, since the input is an $N^2 \times 1$ vector, the network is mainly composed of FC layers. On the one hand, such a design can reduce the size of input data, which is only one-third of the input size adopted by the CNN structure in [43]. Moreover, the parameters of the network will be reduced accordingly, speeding up the training and calculation. At the same time, due to the characteristics of the covariance matrix, there is almost no information loss. On the other hand, the research in [41] has proved that a good estimation result can be obtained on the grid with 1° resolution through several FC layers, so a similar design is adopted for the first part of the network. As shown in Figure 3, in the first part of the network, we used an N^2-dimension input layer, which takes the preprocessed covariance matrix as the input. Then, five FC layers are used to learn the features and output the estimation result on the grid, the output can be expressed as

$$\boldsymbol{z}_1 = f_1(\cdots f_5(x_1)), \tag{13}$$

where $\boldsymbol{x}_1$ represents the input of the first part of the network, i.e., the original input of the network, and each $f(\cdot)$ denotes an FC layer. Thus, the first output is a probability at each entry of the predicted label.

Then, considering that the features of the off-grid part will be more difficult to obtain, we increase the depth of the network and introduce the skip connection. The input of the second part of the network integrates the deep features extracted from the first part of the network, which can be expressed as

$$\boldsymbol{x}_2 = \text{concatenate}(\boldsymbol{x}_1, f_1(\cdots f_4(\boldsymbol{x}_1))), \tag{14}$$

that is to say, the task of the second part of the network is based on the processing results of the first part of the network to a certain extent. It can focus on finding out more accurate target positions near the rough target grid point that has been determined. Finally, another eight FC layers are used to process and output the estimation of the off-grid part

$$\boldsymbol{z}_2 = f_6(\cdots f_{13}(\boldsymbol{x}_2)), \tag{15}$$

the i-th element of output $\boldsymbol{z}_2$ represents the offset between the i-th target and the grid. By combining the outputs of the two networks, an accurate estimation of the target DOAs can be obtained.

It is worth noting that the two parts of the network are trained at the same time, while the second part of the network has deeper layers, and the task training is more difficult. It is necessary to prevent the first part of the network from converging prematurely and generating overfitting in subsequent training. Therefore, two dropout layers are added to the first part of the network to prevent an overfitting problem.

The output layer of the first part adopts Sigmoid activation function $f_{\text{Sigmoid}}(u) = 1/(1 + \mathrm{e}^{-u})$, and thereby returns values in $[0, 1]$. The selection of the Sigmoid function is due to the existence of DOAs of multiple sources, there will be multiple independent output values close to or equal to 1. For the output layer of the second part, we use the identity function, because we want to get the value describing the distance between the signal DOAs and the corresponding grid directly. And ReLU activation function $f_{\text{ReLU}}(u) = \max(u, 0)$ is used in all other layers of the network. Finally, adaptive moment estimation [50] was used to determine the learning rate.

3.4 Computational complexity

For DL-based DOA estimation methods, only simple computations are required to obtain the estimation results after completing model training, indicating a very short run time. In contrast, traditional estimation methods, such as MUSIC, involve complex matrix decomposition so these methods take longer computing time, especially for the practical hardware. Table 1 shows the number of parameters for each

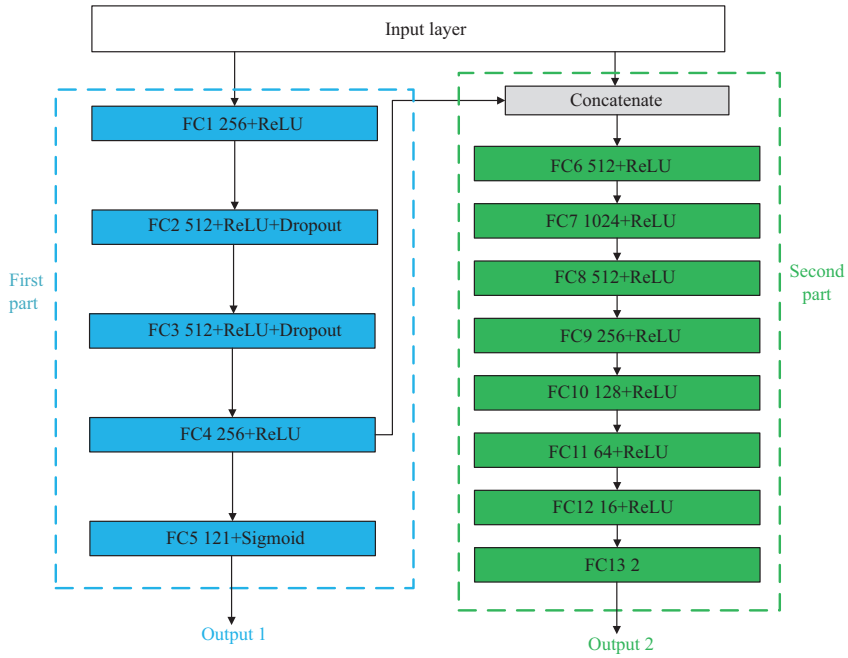

Figure 3 (Color online) Architecture of the proposed network for super-resolution DOA estimation. The network consists of FC layers with the ReLU activation function, except for the two output layers. The first output layer uses the Sigmoid function and the second output layer uses the identity function. The input of the first part is the original input of the network, and the input of the second part is the combination of the original input and the features extracted by the first part. Two dropout layers are employed (for regularization) in the first part of the network.

Table 1 Model complexity and averaged computing time

	Proposed	MUSIC [4]	ESPRIT [5]	SVR [32]	NN [41]	CNN [43]
Total params	1953643	–	–	–	107971	15609721
Test time (s)	$2.95e^{-4}$	$5.67e^{-1}$	$1.22e^{-3}$	$1.74e^{-2}$	$1.85e^{-4}$	$6.42e^{-4}$

DL model and compares the run time of each method. Herein, The resolution of the MUSIC method is set to 0.01°. Each method performs 1000 operations on the same equipment and the time for single estimation is obtained after averaging. As can be seen in Table 1, the proposed method enables faster estimation results compared with other non DL-based methods. Compared with CNN, the proposed method has fewer parameters and not surprisingly realizes a shorter run time. In addition, although the proposed method has a slightly longer run time than the NN method due to the estimation of off-grid errors, this slight difference, regarding the great performance improvement, is acceptable.

4 Experiment result

In this section, we describe the implementation of the proposed network and provide extensive simulation results, where we evaluate the performance of the proposed network in the DOA estimation under various setups. We also compare its performance with other DL-based methods and several traditional methods, including MUSIC [4], ESPRIT [5], SVR in [29,32], DNN in [41], and CNN in [43]. Among them, MUSIC and ESPRIT methods are traditional super-resolution DOA estimation methods, and SVR is a prediction method based on machine learning, which realizes gridless DOA estimation. Finally, DNN and CNN are DL methods, which are still on-grid methods in essence.

4.1 Experiment setup

In both training and testing experiments, we consider a ULA with $N=12$ elements and set the angle-search range to $\phi_{\min}=-60°$ and $\phi_{\max}=60°$. The number of signal sources is set to $K=2$ and the source DOAs are reserved to two decimal places, i.e., accurate to 0.01°, which is the same as that considered in other studies and meets most application requirements. In this context, we will get more than 70 million different angle pairs in total and we need to reduce the training set to facilitate training.

First, we reduce the angle interval to $[1^\circ, 10^\circ)$, because we pay more attention to the performance of the network when the two signal DOAs are very close. Secondly, for each pair of angle intervals, we randomly select 1000 angle pairs for training and obtain 900000 training examples for each SNR. Finally, we use the data obtained from the true covariance matrix in (7) in the training stage, and the estimated covariance matrix in (8) is used in the test stage, because we cannot get the real covariance matrix in practical applications [43]. Also, we set the SNR pattern to stepwise growth, i.e., $\{0, 5, 10, 15, 20, 25, 30\}$ dB. Therefore, we get a training set containing $D = 6300000$ samples. In the case of untrained angle pair and SNRs, the reason why the setup can be used to reduce the amount of data is that the strong adaptability and stability of the DL network enable it to maintain good estimation performance. The subsequent experimental results also prove this point of view.

During network training, the dataset is randomly divided into training set 90% and verification set 10%. The network was trained for 300 epochs with a min-batch size of 512. In addition, when the validation loss reaches a plateau for 10 epochs, the learning rate is decayed by a factor of 0.7 [43]. Because the output of the first part adopts the sigmoid activation function, and a higher priority to the estimation results of the first part is preferred. The loss weights of the two outputs are set to 100 and 0.1, respectively. The network was implemented in Keras using Tensorflow as the backend. All the experiments are tested on a server with a Ubuntu 18.04 system, an NVIDIA GeForce RTX 3090 GPU, and 512 GB memory.

4.2 DOA estimation results

The proposed network structure and training method have been described in detail. In this subsection, we will present some intuitive results to show the excellent performance of the network and compare the results with five baseline methods. In order to facilitate testing and consider the actual application requirements, the resolution of the MUSIC method is set to 0.01°.

First, in order to test the performance of each method under general conditions, we keep the incident angles of the two signals at a fixed interval and change within the angle search range. The SNR is set to 17 dB and two narrow-band signals in the far field impinge on this array with the angle interval fixed to 3°. The direction of the first source θ_1 varies from -59.65° to 56.35° with an increasing step of 1°, and the second source changes accordingly, so there are 117 samples in total. We used $T = 1000$ snapshots to estimate the covariance matrices. The DOAs predicted by the proposed DNN are shown in Figure 4(a) (the solid line represents the true DOAs) and the corresponding errors are shown in Figure 4(g). In addition, the estimates of MUSIC, ESPRIT, SVR, DNN, and CNN are illustrated in Figures 4(b)–(f) and their errors in Figures 4(h)–(l).

For traditional super-resolution algorithms, MUSIC and ESPRIT have relatively small estimation errors at the cost of high computational complexity. As shown in Figures 4(d) and (j), the result of the SVR method is not so stable, its estimation effect is obviously inferior to the first two methods. However, it can be seen from the figure that compared with the other two on-grid DL methods, the proposed off-grid DOA estimation method has achieved better results after considering the off-grid error, and its performance is very close to the traditional super resolution methods with high computational complexity. As can be clearly seen in Figure 4(g), except that a few sample points have errors close to 1°, the errors in most cases (about 94%) remain between $[-0.2^\circ, 0.2^\circ]$. In contrast, the other two DL-based methods do not process the off-grid part of the signal DOAs, and can only make an estimation with a resolution of 1°. Therefore, they generally show greater error. The estimation error of CNN is the distance between the target angle and the nearest grid point, which is between $[-0.65^\circ, 0.35^\circ]$. Due to the small angle interval of the targets set in the experiment, DNN with a weak ability to distinguish adjacent targets shows greater error. Regarding the occasional large error that occurred for the proposed method, the possible reason is the lack of data in the training set. In order to facilitate the training, only a small part of angle pairs is selected. In addition, it is worth noting that the SNR used for testing does not appear in the training set.

Next, in order to highlight the advantages of the proposed off grid method, it is necessary to reduce the angle change step and observe the estimation effect of each method when the target angles varies between grid points. In order to control the number of samples, it is also necessary to narrow the angle range. We consider two signals with an angular distance of $\Delta\theta = 1.85^\circ$ at SNR = 10 dB. Then, the increasing step of the angles is reduced to 0.01° and the direction of the first signal varies from -2° to 0°, so there are 200 samples in total. $T = 2000$ snapshots are used to estimate the covariance matrix. The DOA estimations of the proposed network, MUSIC, ESPRIT, SVR, DNN, and CNN are depicted in Fig-

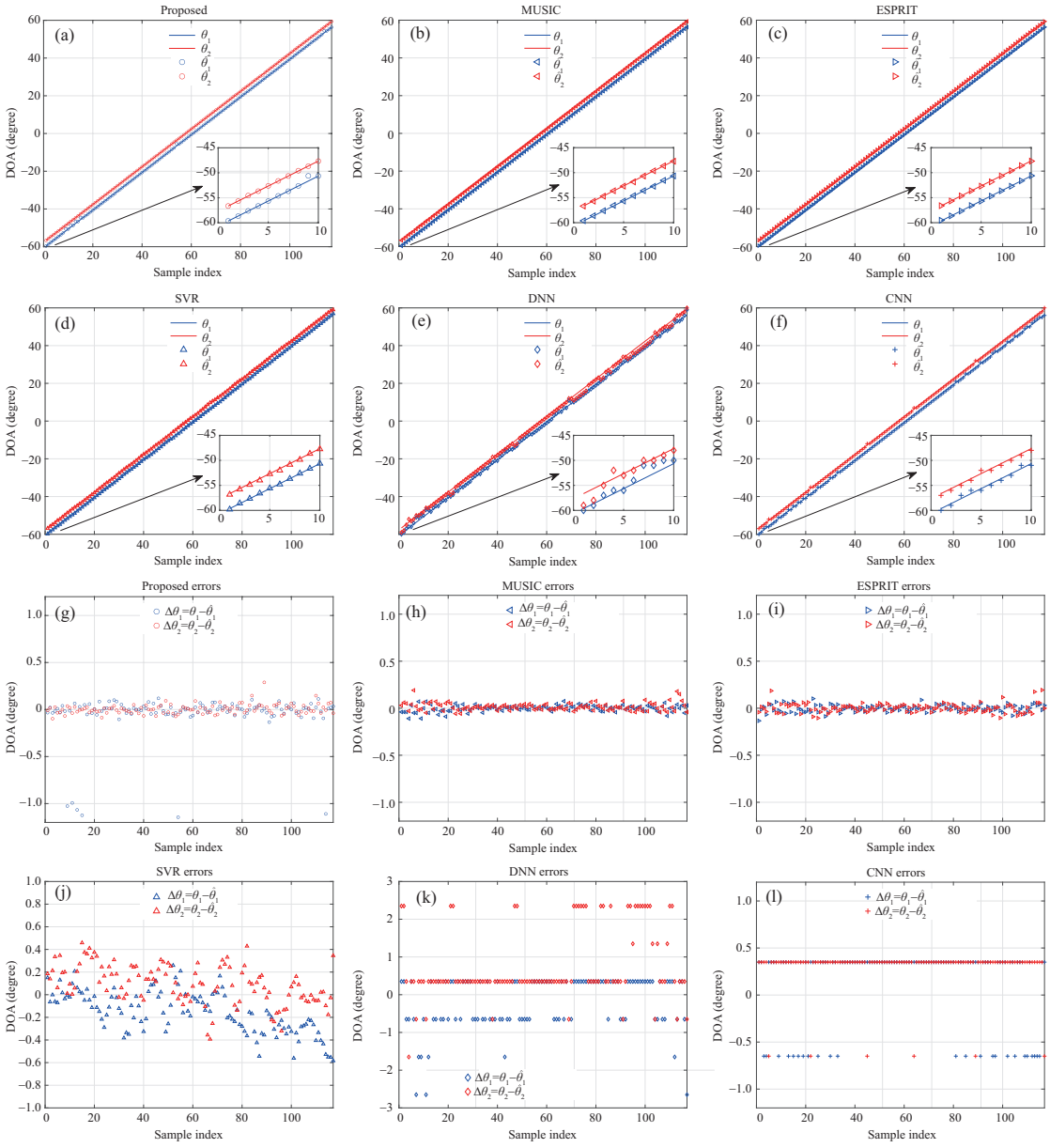

Figure 4 (Color online) DOA estimation performance on angles $\theta_1, \theta_2 \in [-60^\circ, 60^\circ]$ with an angle interval of 3° at 17 dB SNR using $T = 1000$ snapshots. DOA estimates: (a) the proposed, (b) MUSIC, (c) ESPRIT, (d) SVR, (e) DNN, and (f) CNN. The DOA estimation errors of (g) the proposed, (h) MUSIC, (i) ESPRIT, (j) SVR, (k) DNN, and (l) CNN.

ures 5(a)–(f), and their corresponding errors in Figures 5(g)–(l), respectively.

This experiment clearly shows the characteristics and advantages of the proposed network. As can be seen in Figures 5(e) and (f), when the DOAs of the target signals are not exactly on the grid point, the other two DL-based methods do show limitations. Their estimation error is largely affected by grid offset, so they cannot accurately estimate the off-grid target and are not able to achieve the same effect as the MUSIC method and the grid-less ESPRIT, which are shown in Figures 5(b) and (c). On the other hand, the estimation result of the SVR method cannot accurately fit the real angle, as shown in Figure 5(d). However, after adding the processing of the off-grid information, the proposed network shows a significant improvement in DOA estimation. It is closed to the estimation effect of traditional methods, moreover, the amount of calculation is greatly reduced when testing the proposed method. We observe from Figure 5(g) that the errors of the proposed network, which are closed to the results of the ESPRIT method, lie in the interval $[-0.11^\circ, 0.12^\circ]$ in most cases. Its estimation performance will not be affected by the off-grid error, and it can achieve DOA estimation of off-grid targets, while a few sample points with large relative deviation may be due to limited training samples. In addition, the errors of the CNN method [42]

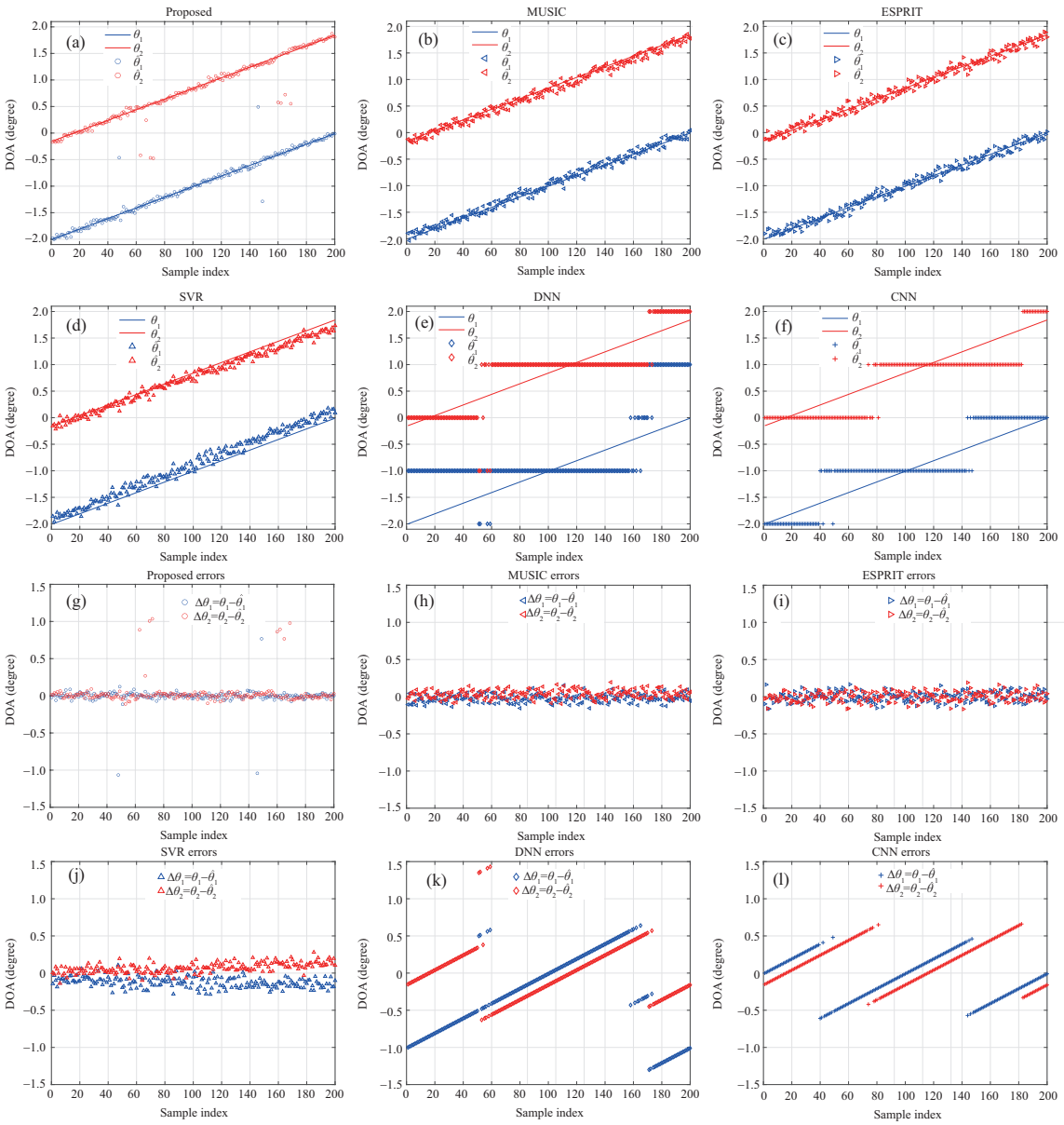

Figure 5 (Color online) DOA estimation performance on angles $\theta_1, \theta_2 \in [-2^\circ, 2^\circ]$ with an angle interval of 1.85° at 10 dB SNR using $T = 2000$ snapshots. DOA estimates: (a) the proposed, (b) MUSIC, (c) ESPRIT, (d) SVR, (e) DNN, and (f) CNN. The DOA estimation errors of (g) the proposed, (h) MUSIC, (i) ESPRIT, (j) SVR, (k) DNN, and (l) CNN.

lie in the interval $[-0.61^\circ, 0.65^\circ]$, and the result of the DNN method is worse, so the effect of the proposed method is the best among these DL-based methods.

4.3 Statistic performance

In the second experiment, we use the average root-mean-square error (RMSE) of all incident signals to evaluate the statistic performance of all methods. The RMSE is defined as follows:

$$\mathrm{RMSE} = \sqrt{\frac{1}{KM}\sum_{k=1}^{K}\sum_{m=1}^{M}\left(\hat{\theta}_k^{(m)} - \theta_k^{(m)}\right)^2}, \tag{16}$$

where $[\hat{\theta}_1^{(m)}, \ldots, \hat{\theta}_K^{(m)}]^{\mathrm{T}}$ are the estimated DOAs of the m-th testing samples, and $[\theta_1^{(m)}, \ldots, \theta_K^{(m)}]^{\mathrm{T}}$ are the true DOAs, M is the repeated number of the Monte-Carlo simulations and K is the number of sources. Furthermore, we set the resolution of the MUSIC method to 0.1° and 0.01° for comparison, named as 0.1° and 0.01° MUSIC method, and two basic experiments are presented in this subsection.

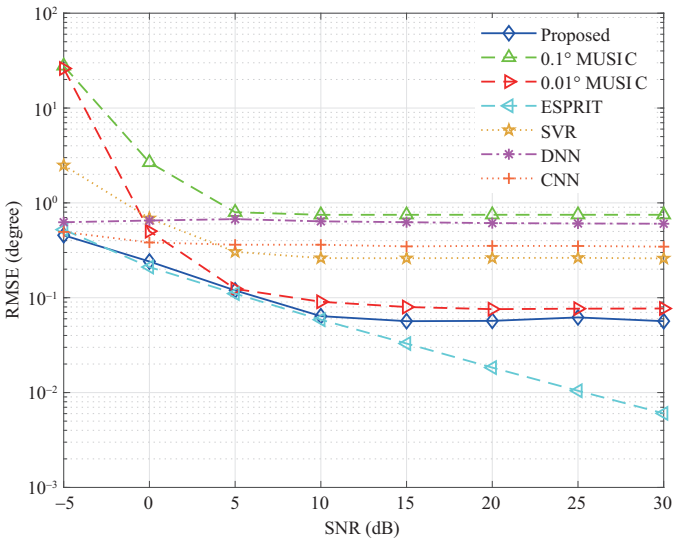

Figure 6 (Color online) RMSE versus SNR in the DOA estimation of two sources by using $T = 1000$ snapshots.

4.3.1 *RMSE results versus different SNRs*

First, two sources, located at the directions 20.33° and 23.68° are considered and the SNR conditions are varying in the range of $[-5, 30]$ dB. At each SNR level, the RMSE is calculated over $M = 1000$ independent simulations and the sample covariance matrix is estimated by using $T = 1000$ snapshots. Then the RMSE versus SNR curve is plotted in Figure 6. As can be clearly observed that the effect of the SVR method is relatively poor among these methods, and its performance does not improve significantly with the increase of SNR. On the contrary, the proposed method shows the best performance in the case of low SNRs, which is the same as the ESPRIT method. With the improvement of SNR, the estimation performance of the proposed method is always better than the SVR method and the other two DL-based methods. Among them, the other two methods based on DL are far worse than the 0.01° MUSIC method. However, due to the processing of the off-grid part of signal angles, the proposed network can finally achieve better performance than the MUSIC method with 0.01° resolution. In general, although the proposed method has an error floor in high SNR, its performance has significantly improved compared with previous DL-based methods. Due to the data-driven characteristics of neural networks and the presence of noise, the output results cannot perfectly fit the true values. When the model completes training, there would be an error between its prediction results and labels, resulting in the upper limit of its performance. When the model reaches this upper limit as SNR increases, it is difficult to show further improvements. However, the accuracy of the proposed method can already meet most practical application requirements. Although the ESPRIT method does not have an error floor, it requires sub arrays with the same shape, which greatly limits the applicable array configurations.

4.3.2 *RMSE versus the number of snapshots T*

In this context, we attempt to estimate the DOAs of two sources at 20 dB SNR while the number of snapshots T varies from 10 to 2000. For each value of T the RMSE is averaged over 1000 simulation runs. The directions of the first and the second sources are $-7.27°$ and $-5.84°$, respectively. In Figure 7, the proposed method shows unique advantages when the number of snapshots is small. It is observed that when 20 snapshots are used to generate test data, the RMSE of the proposed method can be reduced to about 0.23. Moreover, when the number of snapshots increases to 2000, the RMSE decreases to about 0.01. When the number of snapshots is relatively small, the proposed method demonstrates a robust performance even compared with the traditional methods, such as the MUSIC method. In addition, when the number of snapshots becomes large, its performance is significantly better than all other methods. In general, the proposed network shows the best performance, stability, and robustness in the case of limited snapshots among all the mentioned methods, and will be better improved with the increase of the number of snapshots.

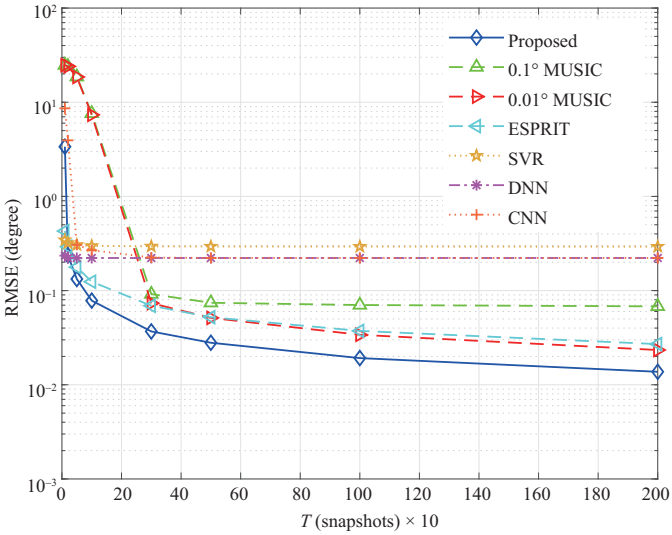

Figure 7 (Color online) RMSE versus the snapshot T in the DOA estimation of two sources from -7.27° and -5.84° at 20 dB SNR.

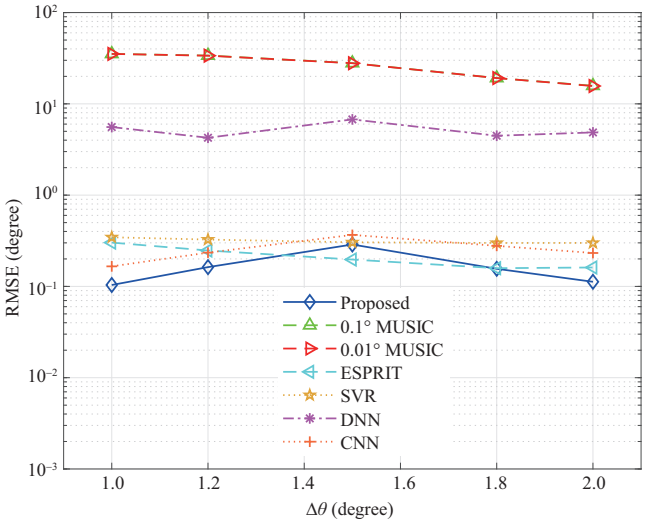

Figure 8 (Color online) RMSE versus the angle interval $\Delta\theta$ at 20 dB SNR.

4.3.3 *RMSE versus the angle interval* $\Delta\theta$

Finally, in order to further verify the super-resolution performance of the proposed method, we test the case that when the arrival directions of two targets are very close, in which the angle interval is set to $\Delta\theta = [1^\circ, 1.2^\circ, 1.5^\circ, 1.8^\circ, 2^\circ]$. For each angle interval, we randomly select 1000 angle pairs for testing, where the angle of the first source θ_1 is within the range $[-60^\circ, 60^\circ - \Delta\theta]$ and the angle range of the second target is $\theta_2 = \theta_1 + \Delta\theta$. The RMSE simulation result at SNR = 20 dB with $T = 100$ snapshots is shown in Figure 8. It can be seen from the results that the MUSIC method cannot accurately estimate DOAs at such a small angle interval, and the same is true for the DNN method. After that, the SVR method is superior to the previous two methods and can estimate the targets adjacent to two angles with an error of about 0.3°. Finally, the proposed method, CNN method, and ESPRIT method can make accurate estimation under several small angle intervals. The performance of the proposed method is better than the CNN method, and the overall error is slightly lower than the ESPRIT method.

4.4 DOA estimation experiment with real data

In this part, we use the measured data collected by Texas Instrument (TI)'s AWR2243 evaluation board to train and test the proposed method, DNN and CNN, and compare the estimation results with traditional

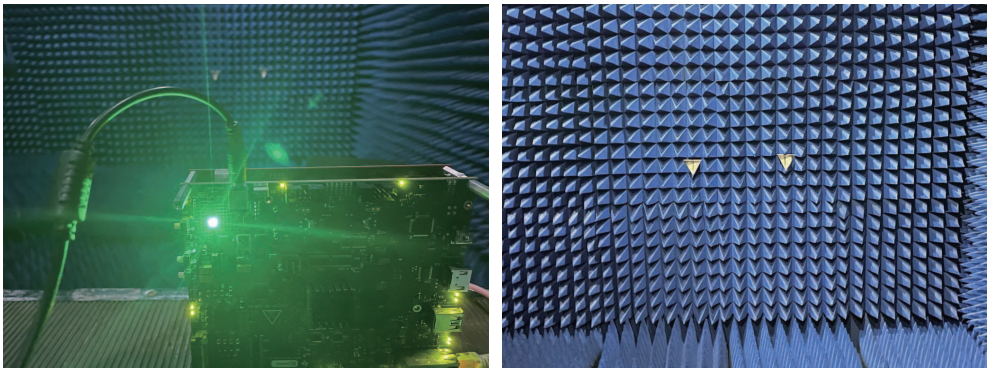

(a) (b)

Figure 9 (Color online) Experimental equipment and environment. (a) TI's AWR2243 evaluation board; (b) corner reflectors.

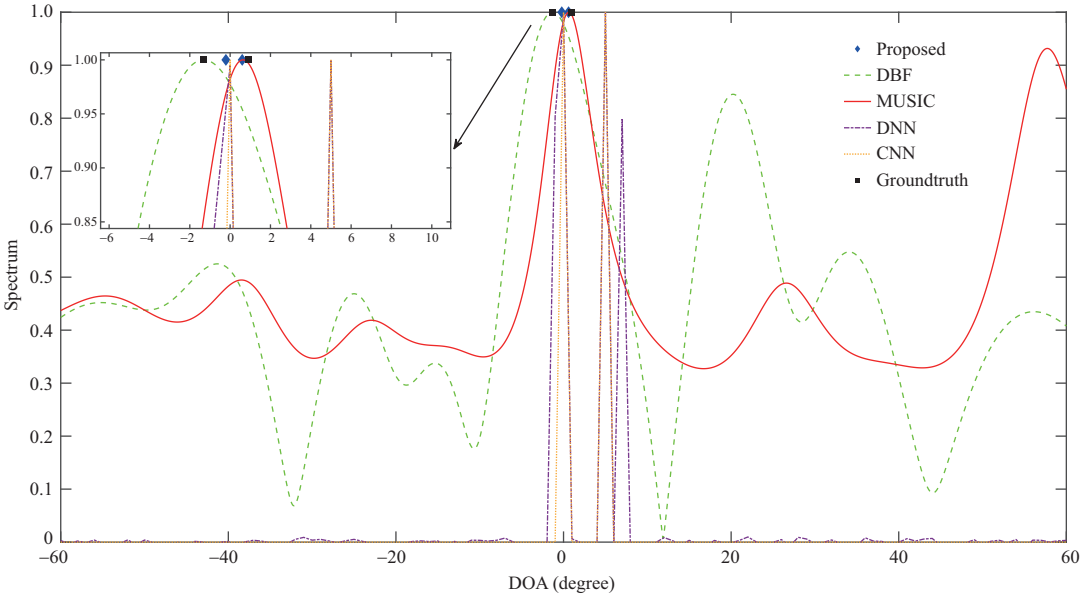

Figure 10 (Color online) Estimation results of two targets with real data.

DBF (digital beam forming) and MUSIC methods. Among them, DBF and MUSIC are commonly used DOA estimation methods in practical applications, while DNN and CNN are both DL-based methods as the proposed methods. The experimental equipment and environment are shown in Figure 9. We adopted 3 Tx and 4 Rx for all collected data such that the resulting virtual array consists of $N = 12$ elements. The angle resolution processing is known to be $\theta_{\text{res}} = \frac{\lambda}{Nd\cos\theta}$. For boresight $\theta = 0°$, $N = 12$ and $d = \frac{\lambda}{2}$, the angle resolution is approximated to 9.5°.

We collected 16200 samples in total for three different angular intervals of 5.8°, 7.6°, and 9.8° as training data. And then all the methods are tested under the case that two targets with an interval of 2.2°. This situation is not included in the training data, and theoretically, traditional methods cannot distinguish two targets with such a close interval. The estimation results of each method are shown in Figure 10. The true angles of the two targets are about −1.3° and 0.9°. It can be seen from the figure that the traditional DBF method has only one peak, and it is impossible to distinguish two targets, while the MUSIC method can only approximately estimate the angle of one target as well. For the three DL-based methods, Both DNN and CNN methods estimate two targets, but only one target's estimated value falls between the real angles, and the other has a relatively large deviation, about 5° and 7°, respectively. Finally, the proposed method shows the best estimation performance, it successfully distinguishes two targets and makes the most accurate estimation, of which the minimum error is only about 0.3°. After that, four groups of data with different angle intervals are involved in the training, 75% of which are used as the training set, 25% are used as the test set, and the RMSE performance of the three DL-based methods is shown in Table 2. It can be seen from the table that the stability and accuracy of the proposed

Table 2 A total RMSE of DL methods with real data

$\Delta\theta$	Proposed	DNN	CNN
2.2°	0.50	1.55	0.63
5.8°	0.89	3.18	1.74
7.6°	0.84	5.18	3.16
9.8°	0.58	6.03	0.63

method when tested with real data are higher than those of the other two DL methods.

5 Conclusion

In this paper, a DL network for the DOA estimation of off-grid signals is proposed. We first estimated the DOAs of the signal sources on a 1° resolution grid, which is modeled as a multi-label classification task. Then, we regard the information processing of the off-grid part as a regression task to directly obtain the offset between the true DOAs and the grid. In order to obtain more accurate estimation results, we use skip connections to concatenate the features of the previous part and the original input into a new input to complete this part of the task. Combining the results of the two parts, we can get more accurate DOA estimation results for general signals. Based on the previous experiments, it can be concluded that the proposed network structure can indeed process and extract the characteristics of the off-grid part of the signal DOAs. So compared with other DL-based methods, the proposed framework achieves competitive or even better DOA estimation performance. It not only has the advantage of fast operation of DL-based methods but also greatly improves the upper limit of the estimation resolution.

Acknowledgements This work was supported by National Natural Science Foundation of China (Grant No. 61901112).

References

1 Krim H, Viberg M. Two decades of array signal processing research: the parametric approach. IEEE Signal Process Mag, 1996, 13: 67–94
2 Lan L, Liao G S, Xu J W, et al. Range-angle-dependent beamforming for FDA-MIMO radar using oblique projection. Sci China Inf Sci, 2022, 65: 152305
3 Ge S, Li K, Rum S N B M. Deep learning approach in DOA estimation: a systematic literature review. Mobile Inform Systems, 2001. doi: 10.1155/2021/6392875
4 Schmidt R. A signal subspace approach to multiple emitter location spectral estimation. Dissertation for Ph.D. Degree. Palo Alto: Stanford University. 1981
5 Roy R, Paulraj A, Kailath T. Estimation of signal parameters via rotational invariance techniques — ESPRIT. In: Proceedings of the IEEE Military Communications Conference: Communications-Computers: Teamed for the 90's, 1986. 1–5
6 Rao B D, Hari K V S. Performance analysis of Root-Music. IEEE Trans Acoust Speech Signal Process, 1989, 37: 1939–1949
7 Ottersten B, Viberg M, Kailath T. Performance analysis of the total least squares ESPRIT algorithm. IEEE Trans Signal Process, 1991, 39: 1122–1135
8 Shi B H, Jiang X Y, Chen N, et al. Fast ambiguous DOA elimination method of DOA measurement for hybrid massive MIMO receiver. Sci China Inf Sci, 2022, 65: 159302
9 Qin G D, Bao D, Liu G G, et al. Cross-correlation matrix Root-MUSIC algorithm for bistatic multiple-input multiple-output radar. Sci China Inf Sci, 2015, 58: 1–10
10 Donoho D L. Compressed sensing. IEEE Trans Inform Theor, 2006, 52: 1289–1306
11 Yang Z, Li J, Stoica P, et al. Sparse methods for direction-of-arrival estimation. Acad Press Lib Signal Process, 2018, 7: 509–581
12 Malioutov D, Cetin M, Willsky A S. A sparse signal reconstruction perspective for source localization with sensor arrays. IEEE Trans Signal Process, 2005, 53: 3010–3022
13 Wipf D P, Rao B D. An empirical Bayesian strategy for solving the simultaneous sparse approximation problem. IEEE Trans Signal Process, 2007, 55: 3704–3716
14 Liu Z M, Huang Z T, Zhou Y Y. An efficient maximum likelihood method for direction-of-arrival estimation via sparse Bayesian learning. IEEE Trans Wireless Commun, 2012, 11: 1–11
15 Hu N, Ye Z F, Xu D Y, et al. A sparse recovery algorithm for DOA estimation using weighted subspace fitting. Signal Process, 2012, 92: 2566–2570
16 Ma Y N, Cao X B, Wang X R. Off-grid DOA estimation with arbitrary-spaced linear array using single snapshot. In: Proceedings of the IEEE Radar Conference (RadarConf), Boston, 2019. 1–6
17 Ling Y, Gao H T, Zhou S, et al. Robust sparse Bayesian learning-based off-grid DOA estimation method for vehicle localization. Sensors, 2020, 20: 302
18 Zhu H, Leus G, Giannakis G B. Sparsity-cognizant total least-squares for perturbed compressive sampling. IEEE Trans Signal Process, 2011, 59: 2002–2016
19 Yang Z, Xie L H, Zhang C S. Off-grid direction of arrival estimation using sparse Bayesian inference. IEEE Trans Signal Process, 2013, 61: 38–43
20 Gretsistas A, Plumbley M D. An alternating descent algorithm for the off-grid DOA estimation problem with sparsity constraints. In: Proceedings of the 20th European Signal Processing Conference (EUSIPCO), Bucharest, 2012. 874–878
21 Duan H P, Qian Z G, Wang Y Y. Off-grid DOA estimation based on noise subspace fitting. In: Proceedings of the IEEE International Conference on Digital Signal Processing (DSP), Singapore, 2015. 675–678

22 Zhang Y, Ye Z F, Xu X, et al. Off-grid DOA estimation using array covariance matrix and block-sparse Bayesian learning. Signal Process, 2014, 98: 197–201
23 Liu D H, Zhao Y B. Real-valued sparse Bayesian learning algorithm for off-grid DOA estimation in the beamspace. Digital Signal Process, 2022, 121: 103322
24 Dai J S, Bao X, Xu W C, et al. Root sparse Bayesian learning for off-grid DOA estimation. IEEE Signal Process Lett, 2017, 24: 46–50
25 Wang Q L, Zhao Z Q, Chen Z M, et al. Grid evolution method for DOA estimation. IEEE Trans Signal Process, 2018, 66: 2374–2383
26 Chen T, Shi L, Guo L M. Gridless direction of arrival estimation exploiting sparse linear array. IEEE Signal Process Lett, 2020, 27: 1625–1629
27 Wu S, Yuan Y, Huang L, et al. Grid-less DOA estimation of coherent sources based on the covariance matrix recovery. Phys Commun, 2021, 46: 101345
28 Du J X, Feng X A, Yan M. DOA estimation based on support vector machine — large scale multiclass classification problem. In: Proceedings of the IEEE International Conference on Signal Processing, Communications and Computing (ICSPCC), Xi'an, 2011. 1–4
29 Pastorino M, Randazzo A. A smart antenna system for direction of arrival estimation based on a support vector regression. IEEE Trans Antennas Propagat, 2005, 53: 2161–2168
30 El Gonnouni A, Martinez-Ramon M, Rojo-Alvarez J L, et al. A support vector machine MUSIC algorithm. IEEE Trans Antennas Propagat, 2012, 60: 4901–4910
31 Pan J J, Wang Y D, Le Bastard C, et al. DOA finding with support vector regression based forward C backward linear prediction. Sensors, 2017, 17: 1225
32 Hasan M I, Saquib M. Low complexity single source 2-D DOA estimation based on reduced dimension SVR. In: Proceedings of the 22nd Annual Wireless and Microwave Technology Conference (WAMICON), Clearwater, 2022. 1–4
33 Lo T, Leung H, Litva J. Radial basis function neural network for direction-of-arrivals estimation. IEEE Signal Process Lett, 1994, 1: 45–47
34 LeCun Y, Bengio Y, Hinton G. Deep learning. Nature, 2015, 521: 436–444
35 He K M, Zhang X Y, Ren S Q, et al. Deep residual learning for image recognition. In: Proceedings of the IEEE Conference on Computer Vision and Pattern Recognition (CVPR), Las Vegas, 2017. 6450–6458
36 Liu P F, Qiu X P, Huang X J. Recurrent neural network for text classification with multi-task learning. In: Proceedings of the 25th International Joint Conference on Artificial Intelligence (IJCAI), New York, 2016. 2873–2879
37 Redmon J, Divvala S, Girshick R, et al. You only look once: unified, real-time object detection. In: Proceedings of the IEEE Conference on Computer Vision and Pattern Recognition (CVPR), Las Vegas, 2016. 779–788
38 Zhuang Z H, Xu L, Li J Y, et al. Machine-learning-based high-resolution DOA measurement and robust directional modulation for hybrid analog-digital massive MIMO transceiver. Sci China Inf Sci, 2020, 63: 180302
39 Yao R G, Qin Q N, Wang S Y, et al. Deep learning assisted channel estimation refinement in uplink OFDM systems under time-varying channels. In: Proceedings of the International Wireless Communications and Mobile Computing (IWCMC), Harbin, 2021. 1349–1353
40 Qi C H, Dong P H, Ma W Y, et al. Acquisition of channel state information for mmWave massive MIMO: traditional and machine learning-based approaches. Sci China Inf Sci, 2021, 64: 181301
41 Kase Y, Nishimura T, Ohgane T, et al. DOA estimation of two targets with deep learning. In: Proceedings of the 15th Workshop on Positioning, Navigation and Communications (WPNC), Bremen, 2018. 1–5
42 Wu L L, Liu Z M, Huang Z T. Deep convolution network for direction of arrival estimation with sparse prior. IEEE Signal Process Lett, 2019, 26: 1688–1692
43 Papageorgiou G, Sellathurai M, Eldar Y. Deep networks for direction-of-arrival estimation in low SNR. IEEE Trans Signal Process, 2021, 69: 3714–3729
44 Liu Z M, Zhang C, Yu P S. Direction-of-arrival estimation based on deep neural networks with robustness to array imperfections. IEEE Trans Antennas Propagat, 2018, 66: 7315–7327
45 Ahmed A M, Eissa O, Sezgin A. Deep autoencoders for DOA estimation of coherent sources using imperfect antenna array. In: Proceedings of the 3rd International Workshop on Mobile Terahertz Systems (IWMTS), Essen, 2020. 1–5
46 Gao Y, Xu J, Jia X. Joint number and DOA estimation via the eigen-beam mCapon method for closely spaced sources. Sci China Inf Sci, 2015, 58: 129302
47 Yan F G, Jin M, Zhou H J, et al. Low-degree root-MUSIC algorithm for fast DOA estimation based on variable substitution technique. Sci China Inf Sci, 2020, 63: 159206
48 Elbir A M. DeepMUSIC: multiple signal classification via deep learning. IEEE Sensors Letters, 2020, 4: 1–4
49 Hoang D T, Lee K. Deep learning-aided coherent direction-of-arrival estimation with the FTMR algorithm. IEEE Trans Signal Process, 2022, 70: 1118–1130
50 Kingma D P, Ba J. Adam: a method for stochastic optimization. In: Proceedings of the 3rd International Conference on Learning Representations (ICLR), San Diego, 2014